Influence of Charge Density and Ionic Strength on the Aggregation Process of Cellulose Nanocrystals in Aqueous Suspension, as Revealed by Small-Angle Neutron Scattering

ARTICLE *in* LANGMUIR · APRIL 2015

Impact Factor: 4.46 · DOI: 10.1021/acs.langmuir.5b00851 · Source: PubMed

3 AUTHORS, INCLUDING:

Isabelle Capron
French National Institute for Agricultural Rese…
34 PUBLICATIONS **778** CITATIONS

SEE PROFILE

Langmuir

Article

pubs.acs.org/Langmuir

Influence of Charge Density and Ionic Strength on the Aggregation Process of Cellulose Nanocrystals in Aqueous Suspension, as Revealed by Small-Angle Neutron Scattering

Fanch Cherhal,[†] Fabrice Cousin,[‡] and Isabelle Capron*[,†]

[†]UR1268 Biopolymères Interactions Assemblages, Institut National de la Recherche Agronomique (INRA), F-44316 Nantes, France

[‡]Laboratoire Léon Brillouin, Commissariat à l'Énergie Atomique et aux Énergies Alternatives (CEA) Saclay, F-91191 Gif-sur-Yvette, France

Supporting Information

ABSTRACT: Aggregation of rodlike colloidal particles is investigated here through the aggregation process by either increasing ionic strength or decreasing surface charge density of cellulose nanocrystals (CNCs). The form factor of the nanoparticles is characterized up to the Guinier plateau using small-angle neutron scattering (SANS) extended to very small scattering vector Q. Ionic strength, above the threshold of screening charges, brings aggregative conditions that induced fractal organizations for both charged and uncharged CNCs. These two structures display respective fractal dimensions of 2.1 for charged CNCs at high ionic strength and 2.3 for desulfated CNCs over more than a decade of the scattering vector Q, irrespective of salinity, revealing a denser structuration for neutral particles. This is discussed in the framework of aggregation of rodlike particles with an aspect ratio higher than 8. Furthermore, dilution of the rod gel led to disentanglement of the network of fractal aggregates with a subsequent macroscopic sedimentation of the suspensions, with a characteristic time that depends upon the ionic strength and surface charge density. It revealed a threshold independent of salt content around 2.5 g/L and the metastable out-of-equilibrium character of CNC suspensions.

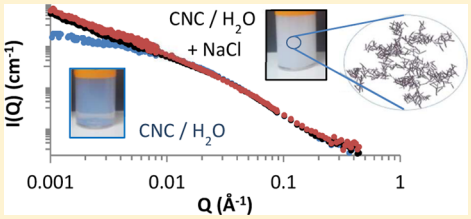

INTRODUCTION

Cotton cellulose nanocrystals (CNCs) are colloidal rod-like particles generally obtained from the sulfuric acid hydrolysis of cotton cellulose fibers.[1,2] It results in highly crystalline rods 100−200 nm long.[3] The elementary crystal dimension has been widely described with a square section of about 5−7 nm using X-ray diffraction.[4,5] However, if the thickness was estimated around 6 nm, such as for individual crystals, it is also described as flat objects constituted of 3−4 laterally bound elementary crystallites with widths over 10 nm.[4,5] It leads to rods with aspect ratios ranging from 8 to 30. The sulfuric acid hydrolysis step also leads to the formation of some ester sulfate groups at their surface. These negative charges induce electrostatic repulsions between CNCs that enable their stabilization in water as aqueous colloidal suspensions at low ionic strength by preventing aggregation induced by attractive van der Waals interactions.[3] A further addition of electrolytes to the suspensions can however destabilize the colloidal stability by screening the electrostatic interactions. The origin of this process can be understood by consideration of the short-range interaction energy between two approaching particles. This can be discussed within the framework of the famous DLVO theory,[6,7] where the interparticle pair potential combines van der Waals attractions and a repulsive Yukawa potential to describe electrostatic repulsions. This potential is mainly determined by two parameters: (i) the total charge of objects and, therefore, their surface charge densities, and (ii) the Debye length κ^{-1}, which is linked to the ionic strength $I = 1/2\sum_i c_i z_i^2$, where c_i is the concentration of ion i and z_i is its valency.[8] Most publications studying the effect of ionic strength have focused on the screening process at very low ionic strength, generally from 0 to 5 mM, varying CNC concentrations between 2 and 40 g/L.[9−12] The Debye length is, in these conditions, always higher than 3 nm, which is a sufficiently large range to counterbalance short-ranged van der Waals attractions and prevent aggregation. Conversely, other studies demonstrated that suspensions were destabilized at electrolyte concentrations higher than 10 mM for Boluk et al. for CNC concentrations of 2.5−10 g/L[10] and electrolyte concentrations of 20 mM for Araki et al. with CNC concentrations of 5−16 g/L,[13] but no systematic study was investigated to describe this aggregation process. Establishing the link between the particle morphology and association mode would be a key parameter to predict their stability in suspension as well as their percolation threshold upon aggregation. In particular, it would allow for the determination if the aggregation mechanisms of CNCs fall within the two main universal processes depicted for colloidal aggregation: the diffusion-limited cluster−cluster aggregation (DLCA)[14] and the reaction-limited cluster−cluster aggregation (RLCA).[15] Both processes lead to aggregates that have an

Received: March 6, 2015
Revised: April 27, 2015
Published: April 28, 2015

DOI: 10.1021/acs.langmuir.5b00851
Langmuir 2015, 31, 5596−5602

internal self-similar structure with a fractal dimension D_f[16−18] which are well-described for spheres interacting with isotropic potential, with DLCA being a fast process, leading to lose and ramified clusters, with a $D_f \approx 1.8$, while RLCA is much slower, promoting more compact clusters, with a $D_f \approx 2.1$. However, processes involving anisotropic particles, such as the CNCs considered here, are less documented. Mohraz et al.[19] probed aggregating Brownian rods with aspect ratios varying from 3.9 to 30.1. An increase of D_f from 1.8 to 2.3 was measured with an increase of the object aspect ratio, eliminating the structural distinction between DLCA and RLCA for very anisotropic rods.

In this paper, the fine understanding of the aggregation process of CNCs in aqueous solution was investigated by tuning the two relevant physicochemical parameters of electrostatic interactions, i.e., CNC surface charge density and solution ionic strength. Our experimental strategy was to probe the morphology of CNC aggregates in suspension by small-angle neutron scattering (SANS), a non-destructive scattering technique. This allowed us to obtain a statistical measurement of individual CNCs averaged over the whole suspension and to ensure that the measurement principle does not itself modify the aggregate morphology. Indeed, SANS has already been used to characterize the size and morphology of isolated CNC. First, Terech et al. described longer tunicin using a cylinder model,[20] and later on, Bonini et al. described modified CNCs with a parallelepiped model.[21] However, to the best of our knowledge, the aggregation of CNCs has never been probed by small-angle scattering (SAS) techniques. This comes from the fact that CNCs are large objects that require measurements at scattering vectors that fall in the Q range of light scattering. However, the samples are turbid, limiting the light scattering analysis that would be the best adapted to these particle sizes once aggregated. The use of SAS techniques with lower scattering vectors [small-angle X-ray scattering (SAXS) or SANS] is also tricky because they generally only allow for dimensions below 200 nm to be probed in direct space and are thereby limited to the individual particle. However, recent experimental development of new V-SANS techniques[22] has enabled the Q range of interest (dimensions in real space up to 750 nm) to be reached, allowing for measurements on turbid samples on the relevant spatial scales to probe CNC aggregates. In comparison to X-rays, a high neutron scattering contrast between CNCs and water can be achieved by suspending samples in D_2O, allowing for data acquisition with good statistics in a matter of minutes and because neutrons are completely non-destructive, which prevents any possible concern of sample beam damage. We were, therefore, able to compare neutral and charged cotton CNCs by SANS on an extended Q range, adjusting the curves with a parallelepiped model and follow their limited cluster aggregation upon ionic-strength-induced association.

MATERIALS AND METHODS

Materials. All of the reagents used were of analytical grade (Sigma-Aldrich), and water was purified with the Milli-Q reagent system (Millipore). CNCs were obtained from Whatman filters (grade 20 Chr). A caliper has been used to measure the volume fractions in tubes without moving the suspensions, and several trials have been previously carried out to check with real volumes.

Sulfated CNCs. CNCs were prepared using sulfuric acid hydrolysis at 58% at 70 °C under stirring for 20 min.[5] After hydrolysis, the suspension was washed by centrifugation, dialyzed to neutrality against Milli-Q water, and deionized using mixed bed resin (TMD-8). The final dispersion was sonicated with a pulse at an amplitude of 30% for 10 min (ultrasonic Qsonica Q700, Misonix, Inc., Farmingdale, NY), filtered, and stored at 4 °C. For conductometric titrations, 10 mL of a CNC suspension in water (0.1%, w/v) was titrated with 10^{-3} mM NaOH using a TIM900 titration manager and a CDM230 conductimeter equipped with a CDC749 titration cell (Radiometer, Denmark). A surface charge density of 0.16 e/nm^2 was determined as usually found following this protocol. Previous transmission electron microscopy (TEM) results gave respective dimensions of 156 nm in length and 15 nm in width.[23]

Desulfation of the Sulfated CNCs. The desulfation of the sulfated CNCs was performed by mild acidic treatment according to a previously described protocol.[5] A total of 300 mL of 5 N HCl was added to 300 mL of 8 g/L sulfated CNC dispersion in a sealed vessel. After hydrolysis, the suspension was washed by centrifugation, dialyzed to neutrality against Milli-Q water, and deionized using mixed bed resin (TMD-8). The final dispersion was sonicated for 10 min, filtered, and stored at 4 °C. Conductometric titration with NaOH showed no negative slope, indicating no detectable sulfate, although traces of weak acid may be detected by a short delay of positive slope (<0.01 e/nm^2).[23] Similar crystalline dimensions and crystallinity to the charged CNCs were also determined (see Table SI-1 of the Supporting Information).

SANS Measurements. SANS measurements were carried out to obtain information on the form factor of the CNCs in various non-aggregating and aggregating conditions. All samples were extensively dialyzed against D_2O to obtain the best possible contrast as well as to reduce as much as possible the incoherent scattering. SANS experiments were carried out at room temperature on two different spectrometers at Laboratoire Léon Brillouin [Commissariat à l'Énergie Atomique et aux Énergies Alternatives (CEA), Centre National de la Recherche Scientifique (CNRS)] at Saclay to obtain a very broad Q range over more than 2 decades (0.00083−0.44 Å^{-1}). The classical SANS PACE spectrometer was used at three configurations, covering a Q range between 0.0024 and 0.44 Å^{-1} (5 Å at 1 m, 5 Å at 4.7 m, and 17 Å at 4.7 m). The V-SANS TPA[22] spectrometer was used with a single configuration to cover the 0.00083−0.008 Å^{-1} Q range. All samples were systematically freshly sonicated for 10 s and loaded in quartz cells (Hellma) of small path length (1 and 2 mm). The azimuthally averaged spectra were corrected for solvent, cell, and incoherent scattering as well as for background noise.[24] The data were fitted with Sasview software.

To determine the CNC dimensions, several fitting models were tried. As already demonstrated, the form factor of a cylinder was not able to fit the data correctly.[20] Conversely, the form factor of a parallelepiped with a rectangular section, averaged over all space orientations, constituted a perfectly fitting model of the rodlike CNCs. The expression of such a form factor is given by

$$F(Q, a, b, c) = \frac{2}{\pi}\int_0^{\pi/2}\int_0^{\pi/2} \frac{\sin(Qa \sin\alpha \cos\beta)}{Qa \sin\alpha \cos\beta} \times \frac{\sin(Qb \sin\alpha \sin\beta)}{Qb \sin\alpha \sin\beta}\frac{\sin(Qc \cos\alpha)}{Qc \cos\alpha} \sin\alpha \, d\alpha \, d\beta \quad (1)$$

where a expresses the thickness, b expresses the width, and c expresses the length of the CNC parallelepiped.

Given that the three parameters a, b, and c have different distinct sizes, their main influences on the scattering curves were located on different Q ranges, which allows for decorrelation of their effect during fitting to obtain their proper values with confidence: (i) the thickness parameter a essentially tunes the overall shape of the scattering curve in the medium Q range; (ii) the width parameter b essentially plays on the Q value of the onset of appearance of the deviation in the low Q range; and (iii) the length parameter c is more difficult to fit correctly because the Guinier range is hardly obtained for such a parameter. Also, at the high Q values, the computation of the form factor induced oscillations that arise from destructive interferences between neutrons scattered by the edges of the parallelepiped and, therefore, related to the thickness size. However, experimentally, they are not observed,

DOI: 10.1021/acs.langmuir.5b00851
Langmuir 2015, 31, 5596−5602

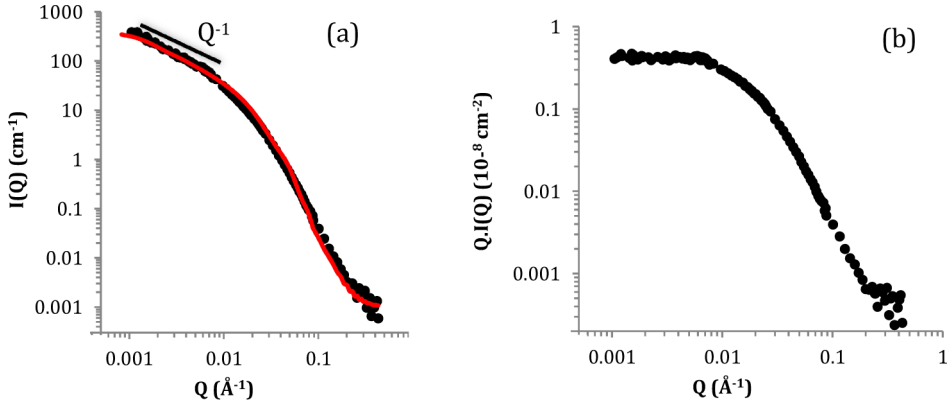

Figure 1. (a) $I = f(Q)$ and (b) $QI(Q) = f(Q)$ representations of the same SANS data for a sulfated CNC suspension in 2 mM NaCl. The red line represents the fit adjusted by the shape of a parallelepiped.

owing to three reasons: (i) convolution by the resolution of the spectrometer ($\delta q/q \sim 10\%$); (ii) CNCs are not all perfectly identical; and (iii) angles of the CNCs are truncated as revealed by X-ray scattering[4] and an *in silico* model.[25] A Gaussian polydispersity of 0.4 on the thickness suppressed these oscillations for all of the samples with increased accuracy on the size parameters. This value was then considered for all samples to take these effects into account.

RESULTS AND DISCUSSION

Form Factor of CNCs. The morphology of individual charged CNCs has first been characterized by SANS. The characteristics measured gave a crystallinity of 82% (see Table SI-1 of the Supporting Information) and a surface density of sulfated groups of 0.16 e/nm^2. Some physicochemical conditions were thus chosen to minimize at most interactions between CNCs, i.e., to remove the structure factor between objects: (i) A low CNC concentration of 7.8 g/L was used. Indeed, in a previous study, Terech et al. did not observe any variation of the shape of the scattering curves at six concentrations of CNC suspensions from 0.7 to 13.7 g/L, considering longer CNCs (from tunicate about 1 μm long), even at the lowest scattering vectors Q probed,[20] indicating that they were probing only a form factor in such a concentration range. (ii) Sulfated CNCs had a charge density of 0.16 e/nm^2. (iii) The ionic strength of the solvent was adjusted to 2 mM by NaCl to decrease the range of electrostatic repulsions, which extend to a very long distance in almost salt-free solutions and may induce a non-negligible structure factor even in such diluted conditions. At the same time, this salinity remains low enough to ensure that electrostatic repulsions between CNCs at a short distance are sufficiently important to prevent their aggregation. In such physicochemical conditions, the scattered intensity of the sample was then considered to arise from the form factor, with the structure factor being considered equal to 1 on the whole Q range. Measurements were performed directly on a freshly sonicated suspension.

Figure 1a shows the scattered intensity $I(Q)$ versus Q profiles of such sample on a Q range lying between 0.000 83 and 0.44 Å^{-1}, which allows us to probe roughly the scales in direct space from 750 nm ($\sim 2\pi/Q_{min}$) down to the nanometer. It shows a Q^{-1} decay at low Q, which is highlighted by the plateau at low Q, on the $QI(Q)$ versus Q representation in Figure 1b. It demonstrates that the CNCs behave as a one-dimensional (1D) rod. This is in accordance with microscopy results performed on dry samples.[23] The Guinier domain is then reached at the lowest Q for what concerns the cross-sectional radius of gyration R_{cross} (with $QR_{cross} < 1$).

The curve was analyzed with a form factor of a parallelepiped with a rectangular section, averaged over all space orientations. The expression of such a form factor given by eq 1 constituted a perfectly fitting model of the CNC curve within error bars. Dimensions of 195 ± 35 nm in length, 22 ± 3 nm in width, and 6 ± 0.2 nm in thickness were obtained. This fitting was very accurate for the thickness (precision was less than a nanometer), good for the width (within a few nanometers), but rather poor for the length, depending largely upon the measurements at the lowest Q, where the signal-to-noise ratio of the data is larger. The thickness of 6 nm is in perfect accordance with the squared cross-section of the elementary crystallites of cellulose determined by X-ray diffraction (see Figure SI-1 and Table SI-1 of the Supporting Information). The width/thickness ratio shows that the mean CNC corresponds to a trimer composed of the lateral association of 3−4 individual crystallites, in accordance with previous studies,[4,5] for which the thickness was maintained at around 6 nm, whereas TEM and cryo-TEM results provided evidence of a larger width of 13−30 nm. The explanation of these lateral associations at a crystalline level is attributed to specific affinities of the different sides of the CNCs.

Ionic-Strength-Induced Aggregation. To follow the aggregation process induced by the increase of ionic strength, SANS measurements were performed on CNC suspensions with the same surface charge density (0.16 e/nm^2) and concentration (7.8 g/L) but with respective salinities of 2, 10, 50, and 200 mM NaCl. Figure 2 shows the variation of the scattered intensity versus the wave vector Q for the four salinities. All of the curves superimpose perfectly at large Q values up to 0.017 Å^{-1} in the range where the scattering is mainly influenced by the thickness of the CNCs (Figure 1a), indicating thicknesses similar to that measured for individual CNCs. When going toward low Q, the scattered intensity increases with increasing salinity, which traduces the formation of associated structures. These aggregates might result from either side-by-side lateral associations of individual CNCs (parallel orientation), in agreement with TEM observations of similar dried systems,[23] or cross-links between either isolated CNCs or small aggregates, resulting from prior lateral associations.

Two cases can be distinguished with respect to salinities. At 2, 10, and 50 mM NaCl, the Guinier regime was reached at low Q. Conversely, at 200 mM NaCl, the typical Q^{-1} decay of a rod-

DOI: 10.1021/acs.langmuir.5b00851
Langmuir 2015, 31, 5596−5602

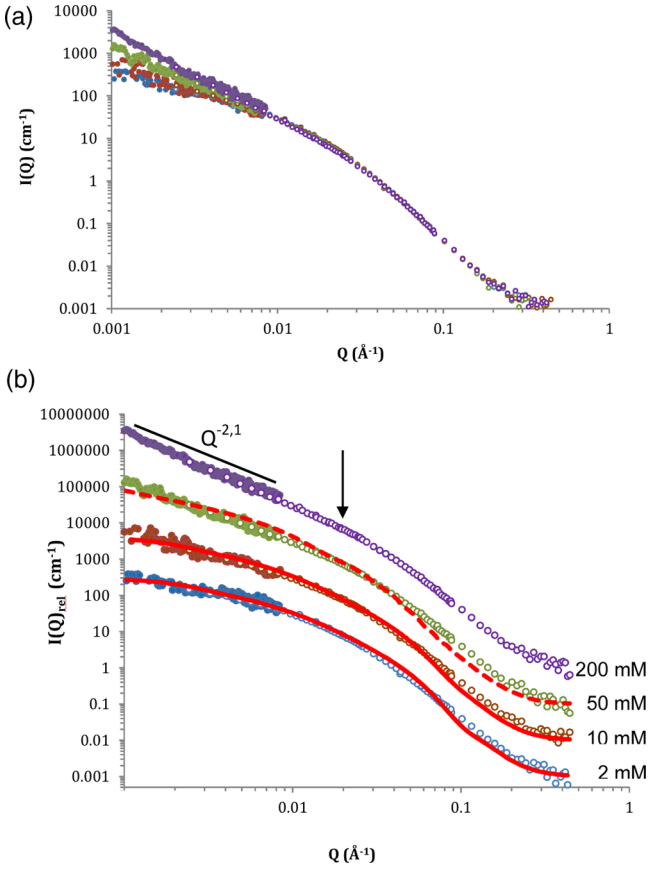

Figure 2. $I = f(Q)$ SANS curves of CNC-sulfated suspensions at 7.8 g/L in 2, 10, 50, and 200 mM NaCl: (a) all scattered curves in absolute scale and (b) curves shifted on the y axis for clarification by a factor of 10 from one curve to another. The arrow indicates the onset appearance of the 2.1 power law dependence for the sample at 200 mM. The continuous lines for the 2 and 10 mM samples are fits with the paralleliped model. The dotted line at 50 mM is a paralleliped model calculation that would give the correct N_{agg} (see the text for details).

like object observed in the low-Q region of the form factor is never reached but a continuous decay with a slope of 2.1 is obtained over more than 1 decade. This slope illustrates the presence of large autosimilar aggregates with a fractal dimension D_f of 2.1 and, therefore, with some branching.

Our SANS measurements enabled us to assess the mean number of aggregation (N_{agg}) of aggregates of isolated CNCs per individual aggregate in suspension at 10 and 50 mM, independent from any fitting, from the interpolation of the scattered intensity at $Q = 0$; $I(Q)_{Q \to 0}$. Such intensity is indeed proportional to the volume of the scattering object, whether it is an isolated CNC or an aggregate of CNCs, according to

$$I(Q)_{Q \to 0} = \Phi \Delta\rho V_{obj} \quad (2)$$

where Φ is the volume fraction of the object and $\Delta\rho$ is the difference of scattering length densities between the object and the solvent. At 2 mM NaCl, $V_{obj} = V_{CNC}$ because CNC nanoparticles are isolated. For the other samples, $V_{obj} = N_{agg}V_{CNC}$, where N_{agg} is the mean number of aggregation. Such N_{agg} can then directly be evaluated for the samples at 10 and 50 mM, through $N_{agg} = I(Q)_{Q \to 0}/I_{sample\ at\ 2\ mM}(Q)_{Q \to 0}$, with respective values of 1.7 and 7.5.

For the sample at 200 mM NaCl, the scattering was still increasing when going toward low Q and it was not possible to obtain $I(Q)_{Q \to 0}$ in our Q window. However, it was possible to make an estimation of the minimum limit value of such a mean aggregation number from the measurement at the lowest experimental Q probed ($N_{agg\ at\ 200\ mM} > 24$). Results are summarized in Figure 3.

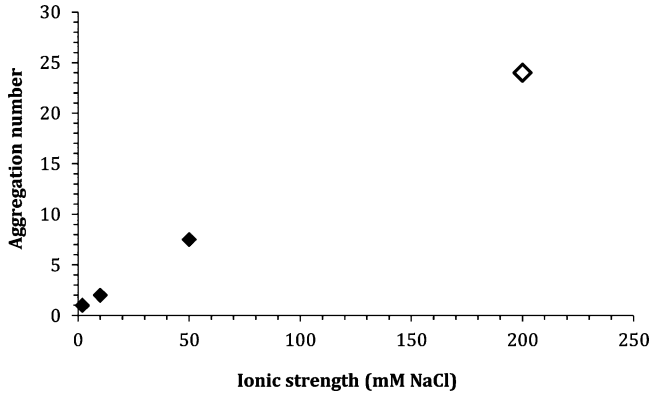

Figure 3. Mean number of aggregation versus the ionic strength of NaCl determined from $I(Q)_{Q \to 0}$ (cm^{-1}). The value for 200 mM NaCl is the minimal limit value of this mean aggregation number.

Such an estimate of N_{agg} was a basis of an attempt to model the scattering curve by the parallelepiped model depicted before, with an increase of either the width and/or the length, given that it fixes the volume of the aggregate. Indeed, a possible fitting by the parallelepiped form factor would mean aggregation through lateral associations, whereas aggregation through branching would not allow for such a modeling. For the 10 mM sample, the modeling was possible (see Figure 2), in accordance with the weak differences observed between its scattered intensity and the intensity of the form factor. The dimensions obtained were 25 ± 3 nm in width and 250 ± 30 nm in length, revealing a slight increase compared to the initial isolated CNC, whereas an unmodified thickness of 6 ± 0.2 nm was recovered. These values give an aggregation number of 1.5 ($25 \times 250 \times 6/22 \times 190 \times 6$), consistent with the N_{agg} of 1.7 defined directly from the intensity at the plateau value. Thus, the aggregation observed at 10 mM may result from moderate associations. Conversely, at 50 mM, it was not possible to model the scattering curve by the parallelepiped model. The best attempt that enables us to recover a N_{agg} of 7.8 and minimize χ^2 between experimental and calculated data is shown in the dotted line in Figure 2. The features of such calculated scattering curve are out of the error bars. It shows, thus, that branching already exists within the aggregates of a few CNCs obtained at such salinity. This is consistent with the large autosimilar and branched aggregates observed when the ionic strength is increased up to 200 mM.

Decreasing Surface Charge Density Using Neutral CNCs. To probe the influence of the surface charge density of CNCs, the same study was performed on the same original CNC sample for which sulfate charges were removed by a post-treatment using HCl. Previous characterization with TEM images of the dried sample revealed associations with an average length of 215 nm and width of 26 nm,[23] but as shown by X-ray diffraction, the crystalline characteristics were preserved, indicating that only the surface was modified (Figure SI-1 of the Supporting Information). The efficiency of such

DOI: 10.1021/acs.langmuir.5b00851
Langmuir 2015, 31, 5596−5602

post-treatment was also characterized by conductometric titration. Although traces of weak acid (likely carboxylic groups) were detected, this sample has been described as neutral CNCs.[23] It led to opaque suspensions, indicating the presence of larger objects. However, no visible sedimentation occurred in the stock suspension at 8 g/L for months, revealing repulsive interactions because of the residual charges.

These neutral CNCs were used for SANS measurements at a constant CNC concentration of 5.4 g/L in three different conditions of salinities: without salt and in 50 and 200 mM NaCl. Figure 4a shows the SANS results for the three

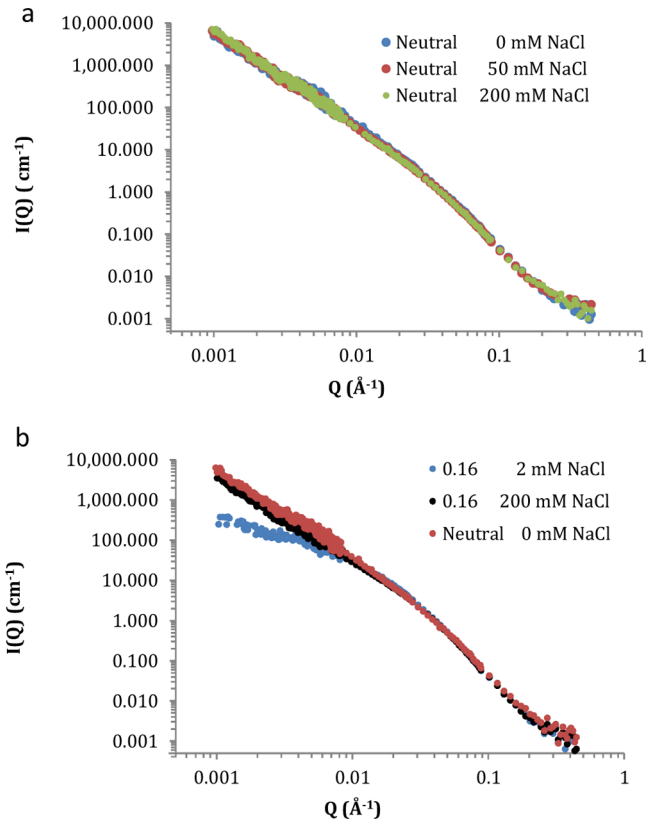

Figure 4. SANS curves of (a) neutral CNC suspensions at 5.4 g/L in pure water and at 50 and 200 mM NaCl and (b) neutral CNCs in water compared to charged CNCs in 2 and 200 mM NaCl.

conditions. It clearly appears that the three scattering curves are identical. No plateau was reached at small Q, and the Guinier regime was clearly outside the Q range probed; however, the scattering curves showed a power-law decay of the scattered intensity as $Q^{-2.3}$. They are compared in Figure 4b to the scattered intensities of the charged CNCs previously depicted at 2 mM NaCl (i.e., the form factor) and at 200 mM NaCl. The scattering curve of the neutral CNCs superimpose to the form factor of an individual CNC at larger Q, but even in absence of ionic strength, an important aggregation of the individual neutral CNCs is observed. The scattered intensity is also higher than in the case of the more aggregated sample with charged CNCs at 200 mM NaCl. The minimum aggregation number of individual CNCs N_{agg} estimated from $I(Q)_{Q \to 0}$ is 53 here. As for the charged CNCs at 200 mM, the CNCs form large autosimilar aggregates. As demonstrated by Figure 5, their fractal dimension D_f of 2.3 is, however, effectively larger than for the charged CNCs with a D_f of 2.1. Given that the density of cellulose of 1.6 g/cm^3 is unchanged, such neutral CNC aggregates are thus denser than the charged CNC aggregates.

Self-Similar Cluster−Cluster Aggregation Process. The structure of the aggregates depicted for neutral and charged CNCs enables us to link the respective influence of the physicochemical parameters on aggregation processes: (i) for charged CNCs, an increase of ionic strength leads to aggregation starting from CNCs at 2 mM with a progressive aggregation state up to 200 mM, while (ii) neutral CNCs strongly aggregate regardless of the ionic strength. The initial morphology is identical because these neutral CNCs originate from the same batch as the charged CNCs, to which a post-desulfation process was carried out. For all of the samples, the SANS curves superimpose at large Q, showing that aggregates are formed with the same building bricks, namely, CNCs with a thickness of 6 nm, in which neither depends upon surface charges nor ionic strength. The striking point concerns the difference of compactness between aggregates from charged and neutral CNCs revealed by their respective fractal dimension of 2.1 and 2.3. These respective D_f values are clearly established in Figure 5 and are in perfect accordance with the mass fractal growth of clusters during the so-called RLCA. In the RLCA model for spherical particles, only a fraction of collisions forms a new aggregate, because an energy barrier has to be overcome prior to forming irreversible bonds. However, the contacts between rod-like objects may involve specific behaviors, because of dispersion or depletion forces that are no longer isotropic, and/or frictional interactions.[26] A crucial parameter is thereby the aspect ratio r, the ratio between the rod length and its cross-section, which determines the effect of the excluded volume interactions on the microstructure. For the charged CNCs, r has a value of 8.9 (on the basis of the length of 195 nm and width of 22 nm obtained from SANS measurements at 2 mM). For neutral CNCs, even if it was not

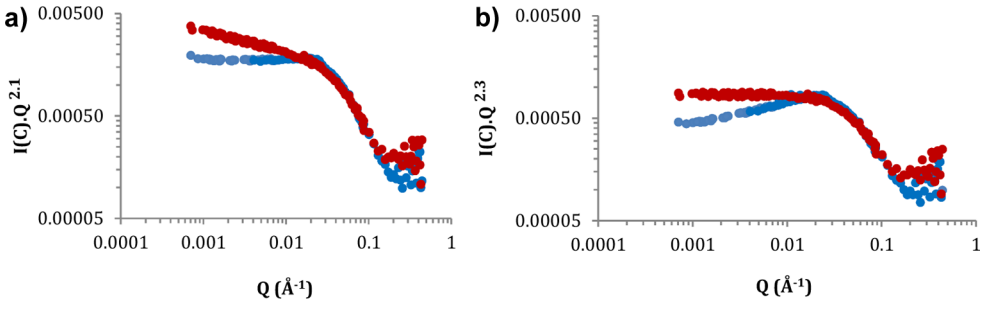

Figure 5. SANS curves of (a) $(I(Q)/C_{CNC})Q^{2.1} = f(Q)$ and (b) $(I(Q)/C_{CNC})Q^{2.3} = f(Q)$ for sulfated CNCs (blue curves) and neutral CNCs (red curves) in 200 mM NaCl.

DOI: 10.1021/acs.langmuir.5b00851
Langmuir 2015, 31, 5596−5602

possible to measure individual objects, the superimposition of the curves at large Q indicates that the aggregates that we observed are formed by CNCs with the same cross-section. The D_f values are in perfect agreement with the results proposed by Morhaz et al., who studied the effect of the aspect ratio on aggregation processes.[19] In their study, they establish that the same D_f value might be reached from both DLCA and RLCA processes when rods have an aspect ratio higher than 8. The general calculation involves interactions between two surfaces as developed in the DLVO theory. Solomon and Spicer stressed that the effect of excluded volume repulsions is the principle determinant of the equilibrium phase behavior leading to heterogeneous fractal clusters.[26] Rods and small rod aggregates have a lower probability relative to spheres of penetrating the structure, because the effective excluded volume per mass unit, driven by the rotational diffusion of a rod, is greater than that of spheres. As a result, the increase in the aspect ratio yields little incremental densification for the slow RLCA process already densely packed, relative to the loose and fast DLCA because of hindered diffusion of the rods. Consequently, it is not possible to differentiate the process as generally defined for RLCA and DLCA. It defines then a general percolation process for rods. A difference in the nature of the interactions is however highlighted by the D_f of 2.3 describing a denser three-dimensional (3D) organization for neutral CNCs compared to 2.1 for charged CNCs. This is attributed to the absence of sulfate groups that increase pair interactions ($U_{contact}$ compared to k_BT), modify the effective excluded volume, and enhance the possibility of denser aggregates. Such associations might be induced by either an increased number of contact points per rod, which leads to denser aggregates, or side-by-side lateral associations at the extremity of the CNCs, leading to elongated particles,[23] which would increase the aspect ratios and D_f, as proposed by Morhaz et al.

We emphasized that the suspensions prepared around 5 g/L in water or 50 mM NaCl were macroscopically homogeneous over a month without visible sedimentation and that neutral CNCs were not sensitive to ionic strength conversely to charged CNCs, whereas a fractal aggregation process is clearly observed by SANS. To investigate this aggregation over time, suspensions at 5 g/L at different salinities were diluted to 0.8 g/L and kept at rest and the turbid fraction of the suspension has been measured over a period of 30 days. It is observed that the suspensions progressively sediment with time (Figure 6). It took a few days for the charged samples with ionic strengths above 50 mM NaCl to observe a clear supernatant, but it took only about 1 day for the neutral samples, as a result of a higher density because they sediment faster. It indicates that the initial suspensions were in a metastable non-thermodynamic equilibrium with weak attractive interactions; otherwise, it would never sediment. It is likely that the concentrations used during the SANS experiments were large enough to enable the formation of a stable percolating network throughout the volume of the vial, whether they have a D_f of 2.1 or 2.3. From the constant volume fraction of the turbid phase reached after sedimentation, we can deduce a limit concentration for which the volume is entirely filled of 2.5 g/L for charged CNCs and 2.3 g/L for neutral CNCs. With a density of 1.6 g/cm^3, the limit volume fraction before a collapse of the gel under gravity that could presumably be a percolation threshold is then of 0.00156 and 0.00144 for charged and neutral CNCs, respectively, positioning them as rod gel.[26] Dilution to a concentration lower than this limit, such as to 0.8 g/L, induces

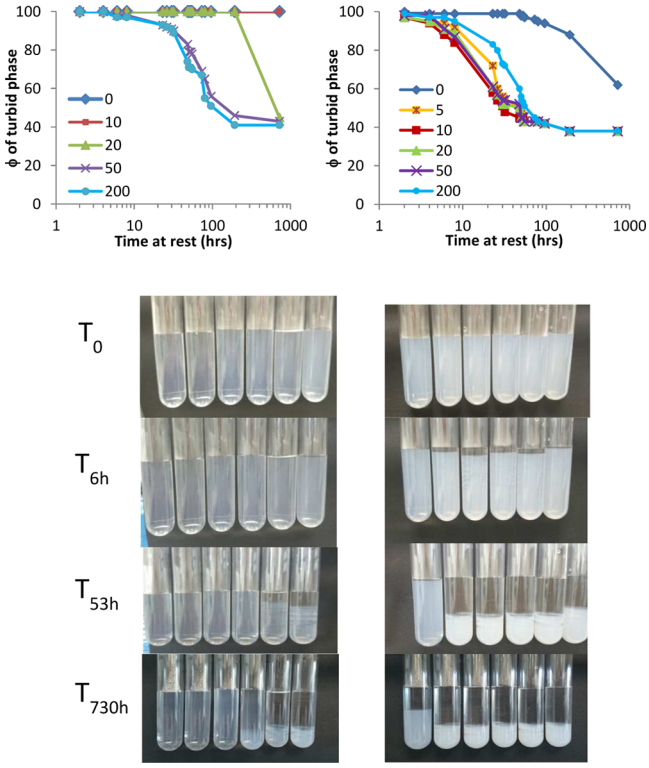

Figure 6. Volume fraction of turbid phase over time for neutral (right) and charged (left) CNCs dispersed at 0.8 g/L and photos of the tubes in 0, 5, 10, 20, 50, and 200 mM NaCl (from left to right).

a partial disentanglement of the scaffold and decreases the aggregate volume fraction below the percolation threshold. In this case, sedimentation occurs. Moreover, the bonds formed between CNCs appeared fragile because they break upon swelling, leading to disruption of the 3D gel. However, there is no indication here whether aggregation occurs or not for charged CNCs below 20 mM NaCl, given that sedimentation is not observed. The charges may not be completely screened, and it takes more time for the particles to associate.

CONCLUSION

This work confirms that CNCs can be modeled efficiently as parallelepiped of mean lateral association of three elementary crystallites, with a thickness corresponding to the squared section of an elementary crystallite (6 nm), as demonstrated by SANS measurements on suspensions of charged CNCs at low ionic strength (2 mM NaCl). When repulsions are decreased or suppressed by either removing charges or increasing ionic strength, a self-similar aggregation process occurs for all samples. Two fractal dimensions are measured: 2.1 for charged CNCs in the presence of ionic strength and 2.3 for neutral CNCs regardless of the ionic strength. These similar values indicate a global open structure for both systems; however, the unambiguous D_f variation reveals a densification of the aggregates when neutral CNCs are used. Furthermore, the aggregation process is fast, appearing as soon as the salt is added. Given that interactions are attractive, the aggregation process will restart as soon as the system is at rest, with a percolation threshold evaluated around 2.5 g/L (volume fraction of 0.0015) for charged CNCs.

DOI: 10.1021/acs.langmuir.5b00851
Langmuir 2015, 31, 5596−5602

■ ASSOCIATED CONTENT

Supporting Information

X-ray diffraction curves (Figure SI-1) and compared crystallinity and crystallographic values for CNCs with different surface charge densities (Table SI-1). The Supporting Information is available free of charge on the ACS Publications website at DOI: 10.1021/acs.langmuir.5b00851.

■ AUTHOR INFORMATION

Corresponding Author

*E-mail: isabelle.capron@nantes.inra.fr.

Notes

The authors declare no competing financial interest.

■ ACKNOWLEDGMENTS

The authors acknowledge Isabelle Grillo [Institut Laue-Langevin (ILL)] and François Muller [Laboratoire Léon Brillouin (LLB)] for their help for modeling and Annie Brûlet (LLB) for her help in V-SANS. Taco Nicolai is also acknowledged for helpful discussion. This work is a contribution to the Labex Serenade (ANR-11-LABX-0064) funded by the "Investissements d'Avenir" French Government program of the French National Research Agency (ANR) through the A*MIDEX Project (ANR-11-IDEX-0001-02).

■ REFERENCES

(1) Revol, J. F.; Bradford, H.; Giasson, J.; Marchessault, R. H.; Gray, D. G. Helicoidal self-ordering of cellulose microfibrils in aqueous suspension. *Int. J. Biol. Macromol.* **1992**, *14* (3), 170−172.

(2) Habibi, Y.; Lucia, L. A.; Rojas, O. J. Cellulose nanocrystals: Chemistry, self-assembly, and applications. *Chem. Rev.* **2010**, *110* (6), 3479−3500.

(3) Araki, J. Electrostatic or steric?—Preparations and characterizations of well-dispersed systems containing rod-like nanowhiskers of crystalline polysaccharides. *Soft Matter* **2013**, *9* (16), 4125−4141.

(4) Elazzouzi-Hafraoui, S.; Nishiyama, Y.; Putaux, J. L.; Heux, L.; Dubreuil, F.; Rochas, C. The shape and size distribution of crystalline nanoparticles prepared by acid hydrolysis of native cellulose. *Biomacromolecules* **2008**, *9* (1), 57−65.

(5) Kalashnikova, I.; Bizot, H.; Cathala, B.; Capron, I. Modulation of cellulose nanocrystals amphiphilic properties to stabilize oil/water interface. *Biomacromolecules* **2012**, *13* (1), 267−275.

(6) Derjaguin, B. V.; Landau, L. Theory of stability of strongly charged lyophobic sols of the adhesion of strongly charged particles in solution electrolytes. *Acta Physicochim. URSS* **1941**, *14*, 633−662.

(7) Vervey, E. J. W.; Overbeek, J. T. G. *Theory of the Stability of Lyophobic Colloids*; Elsevier: Amsterdam, Netherlands, 1948.

(8) Israelachvili, J. N. *Intermolecular and Surface Forces*, 3rd ed.; Academic Press: London, U.K., 2011; p 674.

(9) Araki, J.; Kuga, S. Effect of trace electrolyte on liquid crystal type of cellulose microcrystals. *Langmuir* **2001**, *17* (15), 4493−4496.

(10) Boluk, Y.; Lahiji, R.; Zhao, L. Y.; McDermott, M. T. Suspension viscosities and shape parameter of cellulose nanocrystals (CNC). *Colloids Surf., A* **2011**, *377* (1−3), 297−303.

(11) Hirai, A.; Inui, O.; Horii, F.; Tsuji, M. Phase separation behavior in aqueous suspensions of bacterial cellulose nanocrystals prepared by sulfuric acid treatment. *Langmuir* **2009**, *25* (1), 497−502.

(12) Zhong, L.; Fu, S.; Peng, X.; Zhan, H.; Sun, R. Colloidal stability of negatively charged cellulose nanocrystalline in aqueous systems. *Carbohydr. Polym.* **2012**, *90* (1), 644−649.

(13) Araki, J.; Wada, M.; Kuga, S.; Okano, T. Flow properties of microcrystalline cellulose suspension prepared by acid treatment of native cellulose. *Colloids Surf., A* **1998**, *142* (1), 75−82.

(14) Lin, M. Y.; Lindsay, H. M.; Weitz, D. A.; Klein, R.; Ball, R. C.; Meakin, P. Universal diffusion-limited colloid aggregation. *J. Phys.: Condens. Matter* **1990**, *2* (13), 3093−3113.

(15) Lin, M. Y.; Lindsay, H. M.; Weitz, D. A.; Ball, R. C.; Klein, R.; Meakin, P. Universal reaction-limited colloid aggregation. *Phys. Rev. A* **1990**, *41* (4), 2005−2020.

(16) Kallala, M.; Jullien, R.; Cabane, B. Crossover from gelation to precipitation. *J. Phys. II* **1992**, *2* (1), 7−25.

(17) Fenistein, D.; Barre, L.; Broseta, D.; Espinat, D.; Livet, A.; Roux, J. N.; Scarsella, M. Viscosimetric and neutron scattering study of asphaltene aggregates in mixed toluene/heptane solvents. *Langmuir* **1998**, *14* (5), 1013−1020.

(18) Gummel, J.; Boue, F.; Deme, B.; Cousin, F. Charge stoichiometry inside polyelectrolyte−protein complexes: A direct SANS measurement for the PSSNa−lysozyme system. *J. Phys. Chem. B* **2006**, *110* (49), 24837−24846.

(19) Mohraz, A.; Moler, D. B.; Ziff, R. M.; Solomon, M. J. Effect of monomer geometry on the fractal structure of colloidal rod aggregates. *Phys. Rev. Lett.* **2004**, *92* (15), 155503.

(20) Terech, P.; Chazeau, L.; Cavaille, J. Y. A small-angle scattering study of cellulose whiskers in aqueous suspensions. *Macromolecules* **1999**, *32* (6), 1872−1875.

(21) Bonini, C.; Heux, L.; Cavaille, J. Y.; Lindner, P.; Dewhurst, C.; Terech, P. Rodlike cellulose whiskers coated with surfactant: A small-angle neutron scattering characterization. *Langmuir* **2002**, *18* (8), 3311−3314.

(22) Desert, S.; Thevenot, V.; Oberdisse, J.; Brulet, A. The new very-small-angle neutron scattering spectrometer at Laboratoire Léon Brillouin. *J. Appl. Crystallogr.* **2007**, *40*, S471−S473.

(23) Cherhal, F.; Cathala, B.; Capron, I. Surface charge density variation to promote structural orientation of cellulose nanocrystals. *Nord. Pulp Pap. Res. J.* **2015**, *30* (2), xx.

(24) Brulet, A.; Lairez, D.; Lapp, A.; Cotton, J.-P. Improvement of data treatment in small-angle neutron scattering. *J. Appl. Crystallogr.* **2007**, *40*, 165−177.

(25) Mazeau, K. On the external morphology of native cellulose microfibrils. *Carbohydr. Polym.* **2011**, *84* (1), 524−532.

(26) Solomon, M. J.; Spicer, P. T. Microstructural regimes of colloidal rod suspensions, gels, and glasses. *Soft Matter* **2010**, *6* (7), 1391−1400.

DOI: 10.1021/acs.langmuir.5b00851
Langmuir 2015, 31, 5596−5602